한국동력기계공학회지 제14권 제2호 pp.22~27 2010년 4월

A Numerical Study on the Nozzle Geometry of a Steam Ejector
증기 이젝터의 노즐 형상에 대한 수치해석적 연구

M. K. Ji, Tony Utomo, Z. H. Jin, H. M. Jeong and H. S. Chung
지명국 · 토니우토모 · 김진화 · 정효민 · 정한식

(received 14 May 2009, revised 8 January 2010, accepted 11 March 2010)

주요용어 : 증기이젝터(Steam Ejector), 구동노즐(Primary Nozzle), 혼입율(Entrainment Ratio)

요 약 : 본 논문은 유한체적법에 근거한 CFD 분석기법을 이용하여 증기 이젝터의 성능에 대하여 구동노즐의 기하학적 형상에 따른 영향을 조사하였다. 구동노즐의 직경비를 변화시키고 또한 직경비를 일정하게하고 구동노즐의 위치를 변화시키면서 최적의 조건을 조사하였다. 연구 결과 이젝터의 성능은 구동노즐의 직경과 노즐의 출구 위치에 의해 좌우됨을 확인하였다. 일정 노즐 면적비에 대하여 노즐 목 직경이 감소함에 따라 혼입율이 증가하는 것을 확인하였고 일정 노즐 목 직경에 대하여 면적비의 증가는 혼입율의 감소의 원인이 된다는 것을 확인할 수 있었다. 또한 혼입율은 노즐의 출구 위치에 따라 영향을 받는다는 것도 확인하였다. 혼입율은 노즐 출구의 위치가 이젝터의 상류로 이동할수록 증가하고 그 위치는 이젝터의 일정단면적부 직경(D)에 대하여 0.4D 일 때 최적의 성능을 보였다.

Nomenclature

A : Cross sectional area(m^2)
C_p : Specific heat at constant pressure(J/kgK)
D : Diameter(m)
E : Total internal energy(J/kg)
ER : Entrainment ratio
h : Specific enthalpy(J/kg)
H : Total enthalpy(J)
k : Turbulent kinetic energy(m^2/s^2)
l : Length scale(m)
m : Mass flow rate(kg/s)
NXP : Nozzle exit position
P, p : Pressure(Pa)
T : Temperature(K)
t : Time(s)
u : Velocity in the x-direction(m/s)
V : Volume(m^3)
a : Angle of converging duct(°)
ε : Turbulence dissipation rate(m^2/s^3)
Θ : Angle of mixing chamber entrance(°)
μ : Viscosity(kg/m · s)
ν : Kinematic viscosity(m^2/s)
ρ : Density(kg/m^3)
τ : Shear stress(N/m^2)

정한식(교신저자) : 경상대학교 정밀기계공학과, 해양산업연구소
E-mail : hschung@gnu.ac.kr, Tel : 055-640-3185
지명국 : 영진단조(주) 기술개발부
토니우토모 : Diponegoro Univ. Indonesia
김진화 : 경상대학교 대학원
정효민 : 경상대학교 정밀기계공학과, 해양산업연구소

1. Introduction

Ejectors are used in several different engineering applications such as refrigeration and desalination system[1,2]. Steam ejector performs the mixing and re-compression of two fluid streams (Fig. 1). The fluid with the highest total energy called primary or motive stream (stream 1 in Fig. 1), flows through a convergent divergent nozzle to reach supersonic velocity, creates the low pressure region at the nozzle exit. The secondary or suction stream (stream 2) is drawn into the flow by an entrainment-induced effect and then it is accelerated. A mixing and re-compression of the resulting stream then occurs in a mixing

chamber (converging duct and/or throat), where complex interactions occur between the mixing layer and shocks. In this occurrence, a mechanical energy is transferred from the highest to the lowest energy level, with a mixing pressure lying between the motive or driving pressure and the suction pressure.

A steam ejector used in desalination system (MED-TVC) is an essential part that governs the total process of the overall system. The accurate prediction of the steam ejector performance promotes the reliability of the process and the enhancement of the ejector entraining efficiency improves the performance of MED significantly. It is shown by many researchers that the ejector performance can be further improved through careful design and good manufacturing technique[3-6].

The first rule to obtain maximum performance from a given MED with the ejector system is that it must be operated at the optimum operating conditions. The performance of the system is determined by the ejector primarily. The optimum operating conditions change depending on the ejector geometry, the position of the primary nozzle and the efficiencies of the ejector elements, such as the primary and suction nozzles, the mixing chamber and the diffuser.

It is obvious that a nozzle is the most important part of a steam ejector since it responsible in creating vacuum condition in order to entrain the secondary stream. The ejector performance itself is measured by an entrainment ratio of the secondary stream to primary stream. Hence, a careful design and investigation of nozzle geometry and position in the ejector becomes an important part in obtaining optimum ejector design. In this paper, the investigation is focused on the influence of the primary nozzle geometry and nozzle position on the ejector performance. In this investigation, CFD (computational fluid dynamics) analysis based on the finite volume method is employed.

2. CFD method

The problem under investigation here involved the supersonic flow inside the flow passage of steam ejector. In order to simulate this particular situation, Gambit and FLUENT were used as grid generator and the CFD solver, respectively.

Gambit was used to create the calculation domain and grid elements of the model. The mesh and model was created in a two dimension (2-D) domain. However, the axisymetric solver was applied and therefore, the three dimensional effect (3-D) was taken into account in the simulation. The mesh was made of 24,000 structured quadrilateral elements and later adapted to about 30,000 elements to confirm that the results are grid independent, as shown in Fig. 2. The grid density was concentrated on the areas where significant phenomena were expected.

In the CFD simulation process, suitable turbulence model also plays an important part in order to get the reasonable good results. Along with the grid refinement test, two different turbulence models also tested in this research. The results are illustrated in Table 1.

For an axisymetric turbulent compressible flow, the governing equations of continuity, momentum and energy are solved simultaneously with the constraint, the ideal gas law. The standard k-ε model was selected to model the turbulent viscosity with applying "coupled-implicit" solver. The near wall treatment was left as the "standard wall function", which gave reasonably accurate results for the wall bounded with very high Reynolds number flow.

Boundary conditions of two faces entering a primary nozzle and ejector were set as pressure-inlet, whilst the one leaving ejector was set as pressure-outlet. The values of each boundary were assigned as the saturation properties (temperature and pressure). Since the velocity of the flow entering and leaving the domain was thought to be relatively small compared with the supersonic speed during the

flow process of the ejector; there was no difference between an input of the stagnation pressure and static pressure.

The investigation consists of two parts; first, investigating the influence of nozzle exit position on the ejector performance and secondly, the investigation of the influence of primary nozzle geometries on the ejector performance. The governing equations can be written in their compact Cartesian form as

$$\frac{\partial \rho}{\partial t} + \frac{\partial}{\partial x_i}(\rho u_i) = 0 \tag{1}$$

$$\frac{\partial}{\partial t}(\rho u_i) + \frac{\partial}{\partial x_j}(\rho u_i u_j) = \frac{\partial P}{\partial x_i} + \frac{\partial \tau_{ij}}{\partial x_j} \tag{2}$$

$$\frac{\partial}{\partial t}(\rho E) + \frac{\partial}{\partial x_i}[u_i(\rho E + p)] = \overrightarrow{\nabla} \cdot \left(\alpha_{eff}\frac{\partial T}{\alpha x_i}\right) + \overrightarrow{\nabla} \cdot [u_j(\tau_{ij})] \tag{3}$$

with

$$\tau_{ij} = \mu_{eff}\left(\frac{\partial u_i}{\partial x_j} + \frac{\partial u_j}{\partial x_i}\right) - \frac{2}{3}\mu_{eff}\frac{\partial u_k}{\partial x_k}\delta_{ij} \tag{4}$$

The modelled transport equations for k and ε in the realizable k-ε model are

$$\frac{\partial}{\partial}t(\rho k) + \frac{\partial}{\partial x_i}(\rho u_i k) = \frac{\partial}{\partial x_j}\left[(\mu + \frac{\mu_t}{\sigma_k})\frac{\partial k}{\partial x_j}\right] + G_k - \rho\varepsilon - Y_M \tag{5}$$

$$\frac{\partial}{\partial t}(\rho\varepsilon) + \frac{\partial}{\partial x_i}(\rho\varepsilon u_i) = \frac{\partial}{\partial x_j}\left[\left(\mu + \frac{\mu_t}{\sigma_\varepsilon}\right)\frac{\partial \varepsilon}{\partial x_j}\right] + \rho C_1 S\varepsilon - \rho C_2 \frac{\varepsilon^2}{k + \sqrt{\nu\varepsilon}} + C_{1\varepsilon}\frac{\varepsilon}{k}C_{3\varepsilon}G_b \tag{6}$$

where, $C_1 = \max\left[0.43, \frac{\eta}{\eta+5}\right]$, $\eta = Sk/\varepsilon$

In these equations, C_2 and C_1 are constants. σ_k and σ_ε are the turbulent Prandtl numbers for k and ε, respectively.

The model constants are $C_{1\varepsilon}$ = 1.44, C_2 = 1.9, σ_k =1.0 and σ_ε=1.2. The eddy viscosity is computed from

$$\mu_t = \rho C_\mu \frac{k^2}{\varepsilon} \tag{7}$$

In addition, standard wall functions are considered. Special care is given to the near wall grid, by a local adaptation following $30 \leq y^+ \leq 50$.

Convergence is judged based on simultaneous observation of the scaled residuals and mass flow rate imbalance. The computed mass flow rate imbalance must be at most 0.1% of the mass flow rate at the ejector exit. And all scaled residuals must decrease by three orders of magnitude.

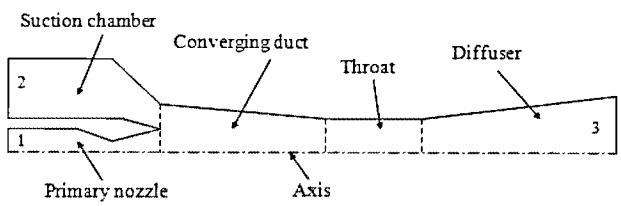

Fig. 1 Typical ejector geometry

Fig. 2 Calculation domain and grid structure of the ejector model

Table 1 Comparison of CFD model to experimental results

Original Cell Number	Turbulence Model	y^+ Wall Treatment	Final Cell Number	ER from CFD Calculation	Error (%)
12,000	Standard $k-\varepsilon$	Non adaption	12,000	0.91	9.6
12,000	Standard $k-\varepsilon$	Adaption	24,000	0.93	12.0
12,000	Realizable $k-\varepsilon$	Adaption	24,000	0.91	9.6
24,000	Standard $k-\varepsilon$	Non adaption	24,000	0.91	9.6
24,000	Standard $k-\varepsilon$	Adaption	30,000	0.92	10.8
24,000	Realizable $k-\varepsilon$	Adaption	30,000	0.91	9.6

Fig. 3 Definition of primary nozzle exit position(NXP)

3. Results and discussion

3.1 The effect of primary nozzle exit position

In this part of investigation, the ejector performance is determined when the nozzle exit position (NXP) is varied at specific operating condition. The definition of NXP is schematically illustrated in Figure 3. The variation of nozzle exit positions are 0.1D, -0.1D, -0.2D, -0.4D, -0.6D, -0.8D, where D is diameter of constant area. The results also contain the basic model of the ejector, where the NXP is at the original location (entrance of mixing duct) as shown also in Fig. 3. The operating condition was set as 2.66 bar for the motive pressure, 0.16 bar for the suction pressure and 0.25 bar for the discharge pressure. The result is shown in Fig. 4.

Fig. 4 illustrates the influence of the nozzle exit position on the entrainment ratio of the ejector. As the nozzle exit position move downstream (+) at a distance of 0.1D, the entrainment ratio is decrease slightly. The reason is obvious. By moving nozzle exit position downstream decreases the effective area. Therefore, the ejector entrains lower secondary fluid while the motive flow rate relative constant, consequently, the entrainment ratio decreases slightly. Conversely, by moving nozzle exit position upstream results in the increase of entrainment ratio.

Apparently, when the nozzle position moves to negative direction of NXP, the effective area is increases; result in the higher intake of secondary fluid. However, the increase of entrainment ratio then reaches one maximum value before subsequently decreases.

The optimum value is obtained when the nozzle exit position is at NXP-0.4D. The decrease is caused by the fact that an increase of effective area also results in higher nozzle exit pressure (Fig. 4). This condition decrease the pressure difference from suction to mixing chamber, hence the driving flow of secondary fluid is decrease. Therefore, the entrainment ratio decreases by further moving nozzle exit position upstream of NXP-0.4D.

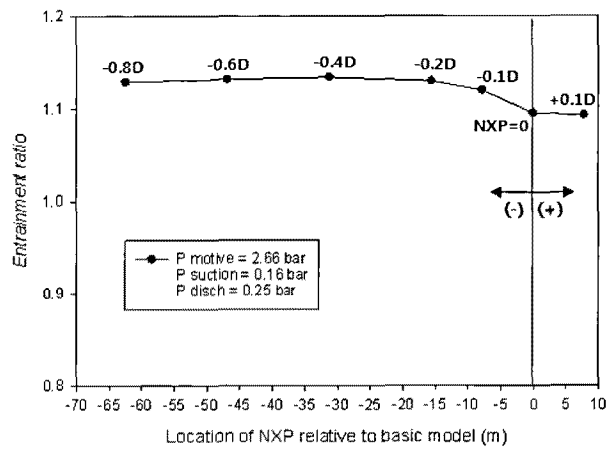

Fig. 4 Effect of primary nozzle exit position on the entrainment ratio

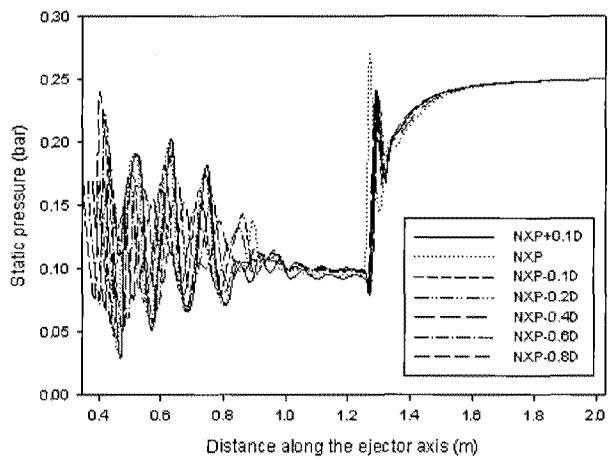

Fig. 5 Effect of primary nozzle exit position on static pressure distributions along the ejector axis

Table 2 Primary nozzle geometries

Model	D_{throat} (mm)	D_{exit} (mm)	Area ratio (A_{exit}/A_{throat})
Nozzle 1	35.4	84.6	5.71
Nozzle 2	36.5	87.2	5.71
Nozzle 3	36.5	77.0	4.45
Nozzle 4	36.5	97.4	7.12
Geometries		D_{throat} ↕	D_{exit} ↕

3.2 The effect of primary nozzle geometries

In this part of investigation, primary nozzle geometries were varied on the nozzle throat and nozzle exit diameter. The operating condition was set constant at specific value. Primary motive pressure, suction pressure and discharged pressure were set as 2.66, 0.08 and 0.18 bar, respectively. The primary nozzle geometries tested are described in Table 2. The result is as shown in Fig. 6.

From Fig. 6, nozzle 1 and 2, it is seen that for a constant area ratio, the entrainment ratio increase with the nozzle diameter. This result appears in contradiction to what have already explain in the previous section. Accordingly, when the ejector equipped with a larger primary nozzle, a larger jet core which has a higher momentum is produced. Therefore a smaller amount of the secondary fluid is allowed to be entrained through the resultant smaller effective area. However, in this investigation, the opposite result is obtained. Since the ejector with smaller primary nozzle operates in the single choking region resulting a lower entrainment ratio than it should be. It can be seen in Figure 7 where at the flow structure of the ejector with nozzle 1, the secondary choking, that is an indication that ejector operate in the double choking region, disappears.

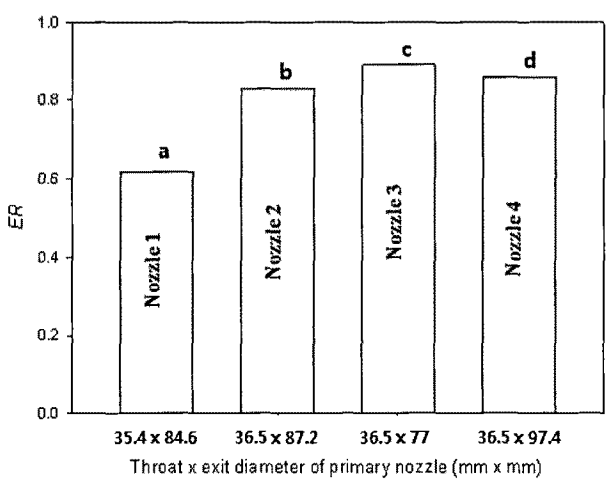

Fig. 6 Effect of primary nozzle geometries on the entrainment ratio

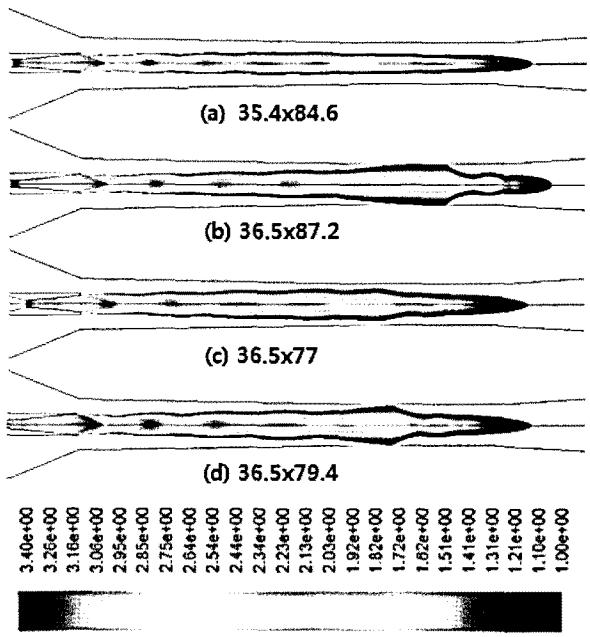

Fig. 7 Effect of primary nozzle geometries on the contour of Mach number

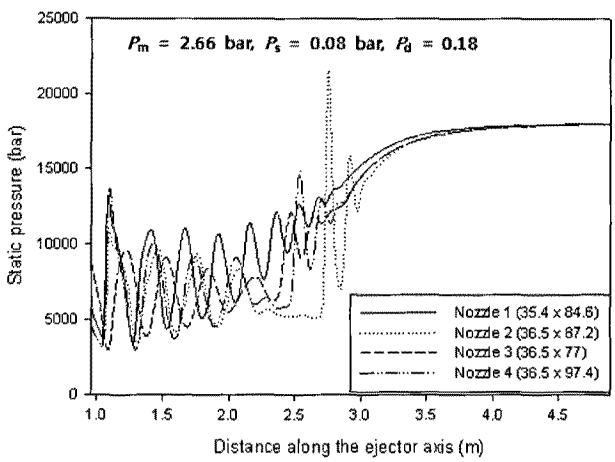

Fig. 8 Effect of primary nozzle geometries on static pressure distributions along the ejector axis

From Fig. 7, nozzle 3 and 4, it is seen that for a constant nozzle throat diameter, the entrainment ratio decreases contrary to the increase of nozzle area ratio (nozzle exit diameter). It can be seen from this figure, the ejector equipped with nozzle which has higher area ratio, yield a larger jet core which has higher momentum. Accordingly, a smaller resultant of effective area is produced, resulting in a smaller amount of the secondary fluid allowed to be entrained.

On the other hand, the total momentum of the

mixed stream increases and a stronger second series of oblique shock can induced as seen in Fig. 8. Therefore, less compression process from the divergent diffuser is needed, and the shocking position moves towards closer to the ejector exit. In conclusion, these flow structures cause a decrease of entrainment ratio. However, an ejector can be operated at a high critical discharge pressure.

4. Conclusions

This study employs CFD techniques to investigate the influence of primary nozzle geometries and nozzle exit position on the ejector performance. The investigation shows that the entrainment ratio of an ejector is influenced by the location of nozzle exit position inside the ejector. The entrainment ratio is increase by moving nozzle exit position upstream direction. However, there is a specific position where the entrainment ratio reaches its maximum value, via at NXP-0.4D, where D is the diameter of constant area throat. The entrainment ratio of an ejector is also influenced by the primary nozzle diameter. At constant nozzle area ratio, the entrainment ratio increases when the nozzle throat diameter is decreases. However, by decreasing primary nozzle throat diameter affect on the decrease of critical discharge pressure. At constant nozzle throat diameter, the increase in area ratio results the decrease of entrainment ratio due to the larger primary jet core produced smaller effective area, hence, smaller amount of secondary flow.

Acknowledgement

This research was financially supported by the Human Resource Training Project for Regional Innovation from Ministry of Knowledge Foundation(KOTEF). The Authors would like to thank Region Strategic Planning Project from Ministry of Knowledge Economy and Brain Korea 21 Project.

Reference

1. Chunnanond K. and Aphornratana S., 2004, "Ejector: applications in refrigeration technology", Renewable & Sustainable Energy Reviews. Vol. 8, pp. 129~155.
2. Park I. S., Park S. M. and Ha J. S., 2005, "Design and application of thermal vapor compressor for multi-effect desalination plant", Desalination, Vol. 182, pp. 199~208.
3. Riffat S. B. and Omer S. A., 2001, "CFD modelling and experimental investigation of an ejector refrigeration system using methanol as the working fluid", Int. J. Energy Res., Vol. 25, pp. 115~128.
4. Huang B. J. et al., 1999, "A 1-D analysis of ejector performance", Int. J. Refrigeration, Vol. 22, pp. 354~364.
5. Dutton J. C. and Carrol B. F., 1986, "Optimal supersonic ejector designs", J. Fluids Engineering, Vol. 108, pp. 414~420.
6. Pianthong K. et al., 2007, "Investigation and improvement of ejector refrigeration system using computational fluid dynamics technique", Energy Conversion and Management, Vol. 48, pp. 2556~2564.
7. FLUENT 6.3 and Gambit 2.4 User's guide, FLUENT INC. Lebanon, NH, USA.